

Energy analysis of a geothermal power plant with thermoelectric energy harvester using waste heat

Mahmut Hekim¹  | Engin Cetin² 

¹Vocational College of Technical Sciences,
Karamanoglu Mehmetbey University,
Karaman, Turkey

²Engineering Faculty, Electrical and
Electronics Engineering Department,
Pamukkale University, Denizli, Turkey

Correspondence

Engin Cetin, Engineering Faculty,
Electrical and Electronics Engineering
Department, Pamukkale University,
Denizli, Turkey.
Email: ecetin@yahoo.com

Funding information

Pamukkale Üniversitesi, Grant/Award
Number: 2017FEBE027

Summary

This study investigates the integration of thermoelectric generators (TEGs) into geothermal power plants to harvest energy from the waste heat and possibly, as a result, to increase the electrical energy generation of geothermal power plants. For this purpose, a model of a geothermal power plant-TEG hybrid system has been designed and implemented as an experimental setup. In addition, the optimized layout configuration of TEGs is obtained by using Matlab & Simulink for 48 pieces of the TEGs. A parametric energy analysis is conducted by varying the temperature of the reinjected geothermal brine and the inlet temperature of the cooling water, since TEGs are planned, so they can be employed between the pipelines of the cooling water and the reinjected geothermal brine. The effects that this has on the performance of the organic Rankine cycle (ORC) and the TEGs are then determined. It was found that the power output of the TEGs increases with the rise in temperature of the reinjected geothermal brine, but the net power of the ORC decreases. For the maximum net power output of the ORC, which is 217.6 kW, TEGs are able to produce 43.42 W for the temperature difference of 41.98°C that corresponds to this status. Therefore, TEGs must be used with lower power outputs to achieve more energy production from this hybrid energy system. For the high inlet temperature values of cooling water, the net power of the ORC decreases, and the power output of the TEGs also goes down. TEGs are able to produce 84.29 W for the temperature difference of 60.6°C for the ORC's maximum net power output of 260 kW. Therefore, it is clear that using TEGs in the power plant for low inlet temperature values of cooling water can be considered. In conclusion, this study demonstrates that waste thermal energy in reinjected geothermal brine can be harvested through TEGs, and this energy could be used to feed the electrical equipment of the power plant with low energy consumptions such as lighting, sensors, instrumentation, and control systems. However, TEGs should be used carefully, since they may affect the overall performance of the geothermal power plant.

KEYWORDS

energy analysis, geothermal energy, geothermal power plant, hybrid system model, thermoelectric generator, waste heat

1 | INTRODUCTION

In recent years, global warming, fluctuations in oil prices, and political crises in different regions where there are fossil fuel reserves have increased the interest in alternative energy sources. Global warming is expected to reach 1.5°C by 2052 if current industrial activities continue.¹ This situation also makes the ongoing trend toward alternative energy sources unavoidable. Although it is believed that, with the COVID-19 global pandemic, energy consumption on a worldwide scale will decrease by 2%,² it will also be inevitable that increases in industrial production will bring a rise in energy consumption values when pandemic conditions are over. Within this context, the ongoing efforts to diversify energy production sources and to get rid of the dependence on fossil fuels will enter a new acceleration era.

The popularization of alternative energy sources coincides with the increase in studies on space and the aftermath of the oil crisis of the 1970s. During this period, intensive research activities were carried out on energy sources such as solar, wind, geothermal, biomass, and hydrogen. Geothermal energy is known to have a special importance among the existing energy production sources. It is used in various sectors such as thermal health, greenhouses, residential heating, and the food industry, as well as in the production of electrical energy. The total installed power of geothermal power plants around the world, which was 8686 MW in 2005,³ reached 13 900 MW by the end of 2019.⁴ In geothermal power plants, the annual global electricity production, which was 52 TWh by 2000, is expected to reach 282 TWh in the year 2030.⁵

The power conversion efficiency of geothermal power plants varies between 10% and 17%.⁶ For this reason, many studies are carried out to increase the efficiency of the geothermal power conversion process. It is seen that the conducted studies have focused on the installation of hybrid systems. Habibollahzade et al.⁷ have established a solar chimney/geothermal system to increase efficiency, thereby increasing the electrical energy production efficiency compared to traditional systems, but achieved a serious decrease in electricity generation costs. Hu et al.⁸ showed that when geothermal power plants are operated as hybrid with solar systems, they are less affected by the temperature changes and reservoir reductions that may occur at the plant site, so they can be operated more efficiently. Ozturk and Dincer⁹ studied a combined cycle geothermal power plant model that produces hydrogen for blending into natural gas to increase energy and exergy efficiencies (with the developed model, energy and exergy efficiencies were obtained as 46.8% and 77.9%, respectively). Heidarnejad et al.¹⁰ investigated a biomass

assisted geothermal power plant that also produces fresh water. The aim of that study is to increase the efficiency of geothermal power plants with low enthalpy by integrating biomass power plants.

Organic Rankine cycle (ORC) enables electricity generation from geothermal sources without the need for high temperature values.¹¹ In ORC, organic working fluid is used in geothermal power plant.¹² There is a heat exchanger in the system and this unit is used to perform the evaporation stages (preheating, vaporization, and superheating).¹³ In the system, the low temperature (<350°C)¹⁴ geothermal fluid transfers its thermal energy through the heat exchanger to the organic cycle fluid that can switch to the vapor phase at low temperatures. Thus, electrical energy can be generated from geothermal reservoirs at low temperatures. The ORC system, which is considered to be a highly efficient system in the production of electrical energy from heat at low temperatures, is a preferred system with its advantages such as flexibility, safety, and low installation cost.^{14,15}

Geothermal power plants with low temperature/efficiency values have been supported with various energy generation systems in order to operate them more efficiently. In addition to biomass, solar energy, and hydrogen energy, there is another power generation system to increase the efficiency of geothermal power plants. It is called thermoelectric generator (TEG). Essentially, waste heat energy from geothermal power plants can be reused for energy generation using TEGs integrated to the geothermal power plant. Waste heat energy is contained in the geothermal fluid, which is sent to the reinjection well after it is used in the production of electrical energy in the geothermal power plant. TEGs are semiconductor devices and generate electrical energy with temperature difference between their two surfaces. TEGs produce electrical energy from waste heat according to the Seebeck effect.¹⁶ One of the most important advantages of TEGs is that they do not have moving parts.^{17,18} This situation facilitates the integration of TEGs into geothermal power plants by reducing operating-maintenance costs.

There are many studies on recovering waste heat from different thermal applications by using TEGs. However, only few of them are about integration of TEGs to geothermal power plants. Actually, geothermal fluid has still some thermal energy before going to the condenser and the reinjection wells. Therefore, the possibilities of using this waste thermal energy should be considered to increase the performance of the geothermal power plants. Niu et al.¹⁹ investigated potential of using TEGs for low-temperature waste heat recovery. They were able to generate 146.5 W with 56 TEGs and a temperature difference between sources of 120°C. Suter et al.²⁰ optimized a 1 kW

thermoelectric stack by simulating different operating parameters and stack geometries considering a 100°C gradient. A heat transfer model coupling conduction through the thermo-element legs with convection to and from the boundary plates was developed by using computational fluid dynamics (CFD) software. Liu et al.²¹ built a system composed by 96 TEGs that generated 160 W with a temperature difference of 80°C. They estimated that this prototype could reach 500 W with a temperature difference of 200°C. Ahiska and Mamur^{22,23} designed a portable TEG of 100 W for low geothermal temperatures. For 67°C temperature difference, the maximum power of 20 TEGs was obtained to be 41.6 W and the conversion efficiency was calculated to be 3.9%. Gholamian et al.²⁴ studied of two different scenarios of using TEGs in geothermal power plants: (i) to employ TEGs for waste heat recovery and (ii) to use TEGs for hydrogen production. The scenarios were modelled and compared from the viewpoints of thermodynamics and exergoeconomics. They obtained that exergy efficiency of the proposed configurations (i) and (ii) was higher than that of the basic ORC by 21.9% and 12.7%, respectively. Also, they mentioned that configuration (i) had the lowest specific product cost. Khanmohammadi et al.²⁵ proposed an integrated geothermal system-based organic Rankine flash cycle with proton exchange membrane fuel cell and TEGs. They modelled the integrated system thermodynamically and compared its results with the conventional system. They found that with using TEGs increases the first and second law efficiencies by 2.7% and 2.8%, respectively. Catalan et al.²⁶ proposed a prototype that utilizes TEGs to generate electrical energy from geothermal sources in shallow hot dry rocky fields. The developed two-phase closed thermosiphon prototype, which includes two TEGs, generates 3.29 W of electrical energy per generator for a temperature difference of 180°C. The study offers loop thermosiphons as a good alternative for generating electrical energy from such geothermal fields due to the low thermal resistance of the system and no auxiliary energy consumption need. Catalan et al.²⁷ designed a system that could be an alternative to traditional geothermal power plants. The proposed system is an energy generation model involving the use of TEGs and heat exchangers together in shallow hot dry rock fields. The designed system was tested in two different prototypes at two different sites. The results obtained that 681.53 MWh of electricity can be produced annually in the geothermal field where the study is carried out with the proposed environmentally friendly model. Neamtu et al.²⁸ proposed a low-power electric generation system with a maximum power point tracker and a Li-ion battery module for electric backup systems. In that system, the TEGs generate electrical energy from the geothermal

brine used for house heating. The simulation results revealed that the proposed model is particularly useful for systems with low power demand, such as security and monitoring systems. Volcanic formations are one of the most important geothermal energy sources. From this point, Catalan et al.²⁹ designed a TEG-based system to meet the energy needs of systems that monitor the activity in volcanic formations. The designed system generated electrical power between 0.32 and 0.33 W per TEG in the reservoir with a temperature range of 69–86°C. Ding et al.³⁰ considered TEGs as a potential alternative for the development of geothermal energy. As a result of their simulation-based study, 136 kW of electrical power was obtained from the TEG for 130°C of geothermal fluid. As a result of the study, it has been shown that the flow rate and temperature of the geothermal fluid have a significant effect on the TEG output power.

All these studies in the literature point out the advantages of using TEGs in geothermal fields. Unlike the others, in this study, integration of TEGs to a geothermal power plant based on ORC is proposed and investigated. TEG hybrid system model is designed using 48 TEGs. This model is designed to be integrated and usable in a real geothermal power plant in its current form, as well as experimentally experiencing such systems in a laboratory environment. Moreover, the effects of utilizing TEGs on power output of the geothermal power plant are found out.

In this study, it is planned to investigate recovering waste heat from the geothermal power plant by using TEGs. Therefore, the main objectives of the study can be summarized as below:

- To obtain optimized layout configuration of TEGs connected in series and parallel.
- To achieve electrical characteristics and performance of TEGs for various flow rates and temperature differences.
- To find out the effects of utilizing TEGs on power output of the geothermal power plant by extending the obtained results from the model and experiments to the real operating data of the geothermal power plant.

For this purpose, an integrated TEG-geothermal power plant is modelled by Matlab & Simulink software, and also an experimental setup is designed. The obtained results from the simulation and the experimental setup are applied to the real-time data of the geothermal power plant installed in Denizli, Turkey. Parametric energy analyses of the geothermal power plant and the hybrid system are done to find out the performance outputs of the geothermal power plant and TEGs. Moreover, integration of TEGs to the geothermal power plant is discussed in terms of its effect on the net power output.

2 | MATERIALS AND METHODS

2.1 | Description of the binary cycle geothermal power plant

General view of the binary cycle geothermal power plant in Denizli, Turkey and its schematic layout are given in Figures 1 and 2, respectively. The binary cycle geothermal power plant works with ORC technology. It consists of a reverse osmosis system, a cooling water pool, cooling towers, a high voltage switchgear cabinet, a 400 kVA transformer cabinet for internal consumers, cooling water pipelines, a step-up transformer, geothermal fluid pipelines, and turbine generator modules.

The geothermal power plant produces electrical energy from geothermal brine with the temperature of nearly 104°C supplied by the production well. In the

geothermal power plant, instead of high pressure steam, a hydrofluorocarbon-based organic working fluid (secondary fluid) containing the chemical compound R245fa (1,1,1,3,3-pentafluoropropane) is used. There is only one production well in the power plant area and the depth of the well is 2400 m. From the production well, approximately 60 kg/s of geothermal fluid can be taken.

Three Pratt & Whitney Pure Cycle 280 modules (turbine generator), each capable of producing 280 kW gross and 260 kW net power, are used to generate electrical energy from the geothermal fluid. The main specifications of the module are presented in Table 1.

The module applies to low temperature (80-160°C) waste heat recovery and power generation, improving the efficiency of energy utilization, and promoting energy conservation and emissions reduction. It has an evaporator, a turbine generator, a condenser, a pump, and an

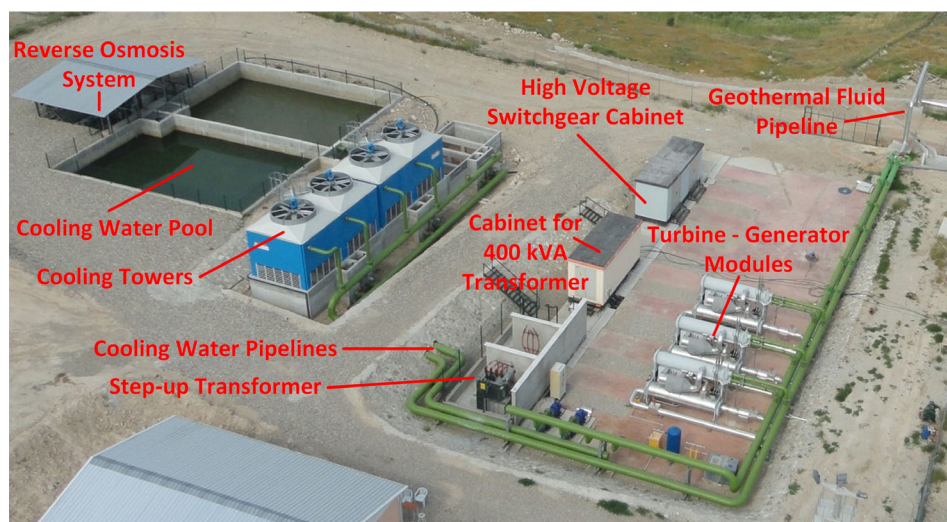


FIGURE 1 General view of the geothermal power plant^{31,32}

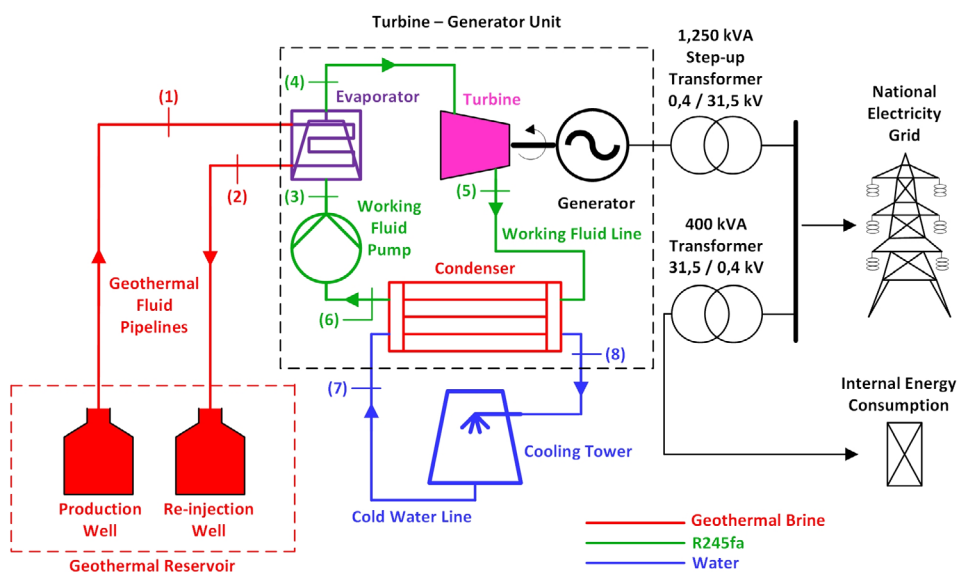


FIGURE 2 Schematic layout of the geothermal power plant

electronic control system. Structure of the module is given in Figure 3. The power plant output voltage is 400 V/50 Hz AC. Electrical energy of 400 V/50 Hz AC generated in the power plant is increased to 31 500 V voltage level with a 1250 kVA step-up transformer. This transformer feeds the national electricity grid. A 400 kVA transformer is used to feed electrical consumers of the power plant. It is a step-down transformer and reduces 31 500-400 V AC voltage level. Thus, the electrical energy generated in the power plant is sent to the national electricity grid.

As seen in Figure 2, in the binary cycle geothermal power plant, the geothermal fluid coming from the production well through pipelines (1) to the Pure Cycle 280 module passes through the evaporator unit (2) and transfers its heat to the organic working fluid (3). The organic working fluid with the superheated-vapor state (4) enables the turbine-generator group to generate electrical energy. After this process, the geothermal fluid used in electrical energy

production is sent to the reinjection well (2) for sustainable energy production. Meanwhile, organic working fluid is sent to the condenser unit (5). The cooling water supplied from the cooling towers which fed by a water pool passes through the condenser (7, 8) and condenses the organic fluid to the liquid state (6). Organic fluid liquefied in the condenser is transferred to the evaporator by the pump. In this way, the closed loop energy generation process continues repeatedly.³³

2.2 | Thermodynamic modelling of the geothermal power plant

Some data are obtained from the geothermal binary cycle power plant in Denizli, Turkey. However, thermodynamic state properties of the ORC cycle working with R245fa are not totally known. Therefore, they should be calculated based on the measured data and several assumptions.

The mass balance for any control volume at steady-state condition is obtained as Equation (1):

$$\sum \dot{m}_{in} = \sum \dot{m}_{out} \quad (1)$$

Based on the first law of the Thermodynamics, energy analysis of any control volume can be expressed by Equation (2):

$$\sum \dot{E}_{in} = \sum \dot{E}_{out} \quad (2)$$

Energy analysis and mass balance equations can be applied on each component of the geothermal power plant.

Temperature-specific entropy (T-s) and temperature-heat transfer diagrams (T-Q) for the evaporator and the condenser, which are heat exchangers, can be useful for calculating the thermodynamic state properties. Figure 4 shows T-s and T-Q diagrams for the binary cycle geothermal power plant. In the T-s diagram (Figure 4A), the upper line represents the behaviour of the geothermal brine while the lower line represents the behaviour of the working fluid. It is obviously seen in the T-Q diagram (Figure 4B) for evaporator that R245fa as compressed fluid in the preheating stage, increases its temperature, and reaches its saturated liquid. Considering the working fluid as a pure substance, once it is heated beyond this point, its temperature remains constant in the evaporation and becomes saturated steam. The minimum difference between the temperature of the geothermal fluid and the working fluid is known as

TABLE 1 Main specifications of Pratt & Whitney Pure Cycle 280 module³³

Properties	Value
Working fluid	R245fa
Maximum rated gross power, kW	280
Maximum rated net power, kW	260
Turbine type	Radial inflow
Generator type	Induction
Power factor (lagging)	>0.95
Hot liquid resource temperature range, °C	80–160

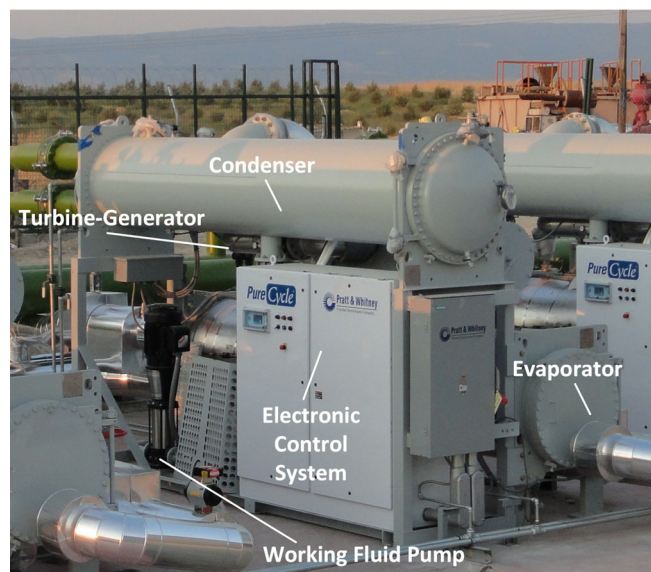


FIGURE 3 Structure of the Pure Cycle 280 module

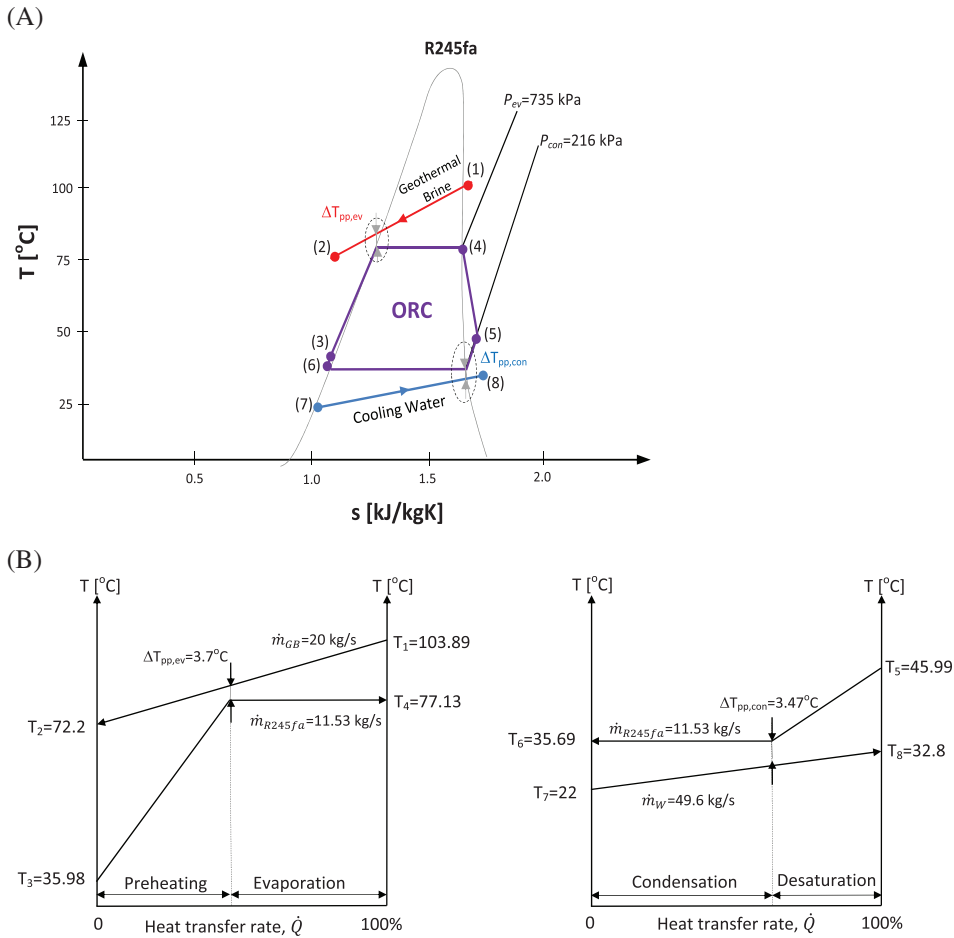


FIGURE 4 A, Temperature-specific entropy diagram for the geothermal power plant for one operating condition at steady state. B, Temperature-heat transfer rate diagrams for pinch point temperature calculations of evaporator and condenser

pinch point for the evaporator, shown as $\Delta T_{pp,ev}$. On the other hand, for condenser, R245fa firstly cools down to its saturated steam state in the desaturation stage and then becomes saturated liquid state. The minimum difference between the temperature of R245fa and water is called as pinch point for the condenser, presented as $\Delta T_{pp,con}$.

For the evaporator, the pinch point temperature and the energy analysis are as below:

$$T_{pp,ev} = T_4 + \Delta T_{pp,ev} \quad (3)$$

$$\dot{m}_{R245fa} \times (h_4 - h_{4f}) = \varepsilon_{ev} \times \dot{m}_{GB} \times (h_1 - h_{pp,ev}) \quad (4)$$

$$\dot{m}_{R245fa} \times (h_{4f} - h_3) = \varepsilon_{ev} \times \dot{m}_{GB} \times (h_{pp,ev} - h_2) \quad (5)$$

Similarly, for the condenser, the pinch point temperature and the energy analysis are calculated as below:

$$T_{pp,con} = T_6 - \Delta T_{pp,con} \quad (6)$$

$$\dot{m}_{R245fa} \times (h_5 - h_{6g}) = \varepsilon_{con} \times \dot{m}_{CW} \times (h_8 - h_{pp,con}) \quad (7)$$

$$\dot{m}_{R245fa} \times (h_{6g} - h_6) = \varepsilon_{con} \times \dot{m}_{CW} \times (h_{pp,con} - h_7) \quad (8)$$

2.3 | The experimental setup

In this study, an experimental setup is designed to investigate how to apply TEGs to geothermal power plants, the stages of generating electrical energy from waste geothermal fluid, and design procedures for such systems. A general view of the setup is given in Figure 5. It can be automatically commissioned by the operator through the Programmable Logic Controller (PLC)-Based Monitoring and Control System (PMCS). Also, according to the values entered by the operator, the fluid temperatures (cold line and hot line) and line pressures in the system can be monitored and adjusted. Data acquisition from the experimental setup is done by the pressure and temperature sensors in the system. First, the data obtained from the sensors come to the analogue modules of the PMCS and then these received data are evaluated by the PLC unit. The experimental setup consists of nine main parts including TEGs, circulation pumps, PMCS, expansion tank, cooler, accumulation tanks, sensors/valves, water lines, and copper profiles, as shown in Figure 5. Water lines connect the main system parts each other and valves are used to adjust the flow of water. The detailed view and list of the main components of the experimental setup are given in Figure 6 and Table 2, respectively.

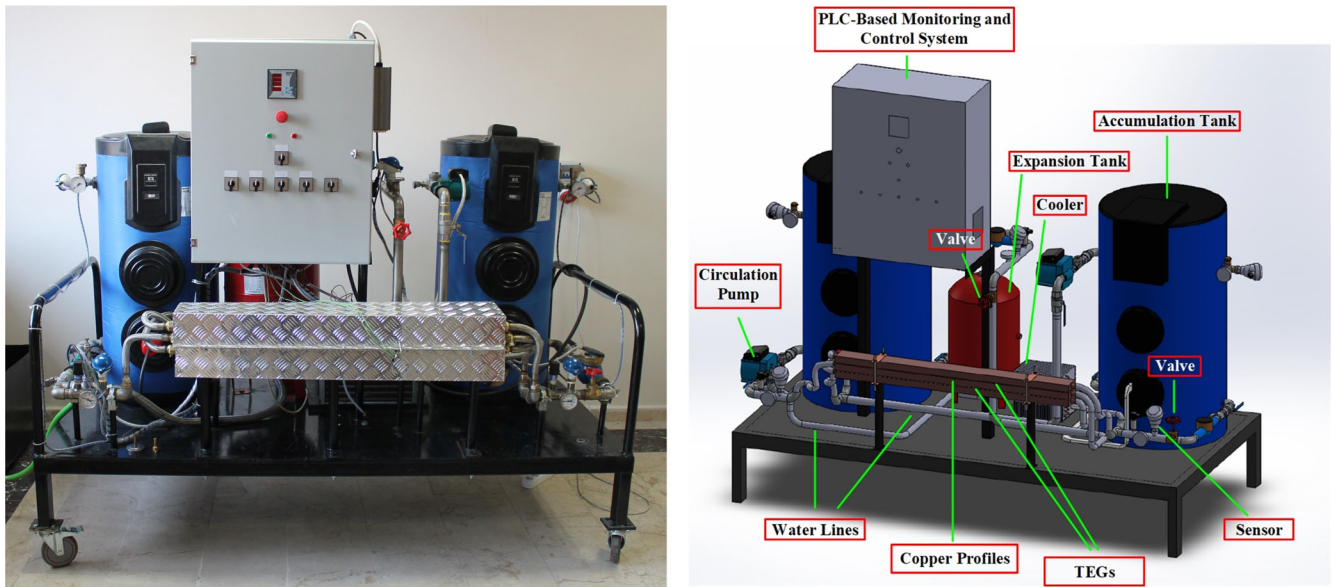


FIGURE 5 General view of the implemented experimental setup

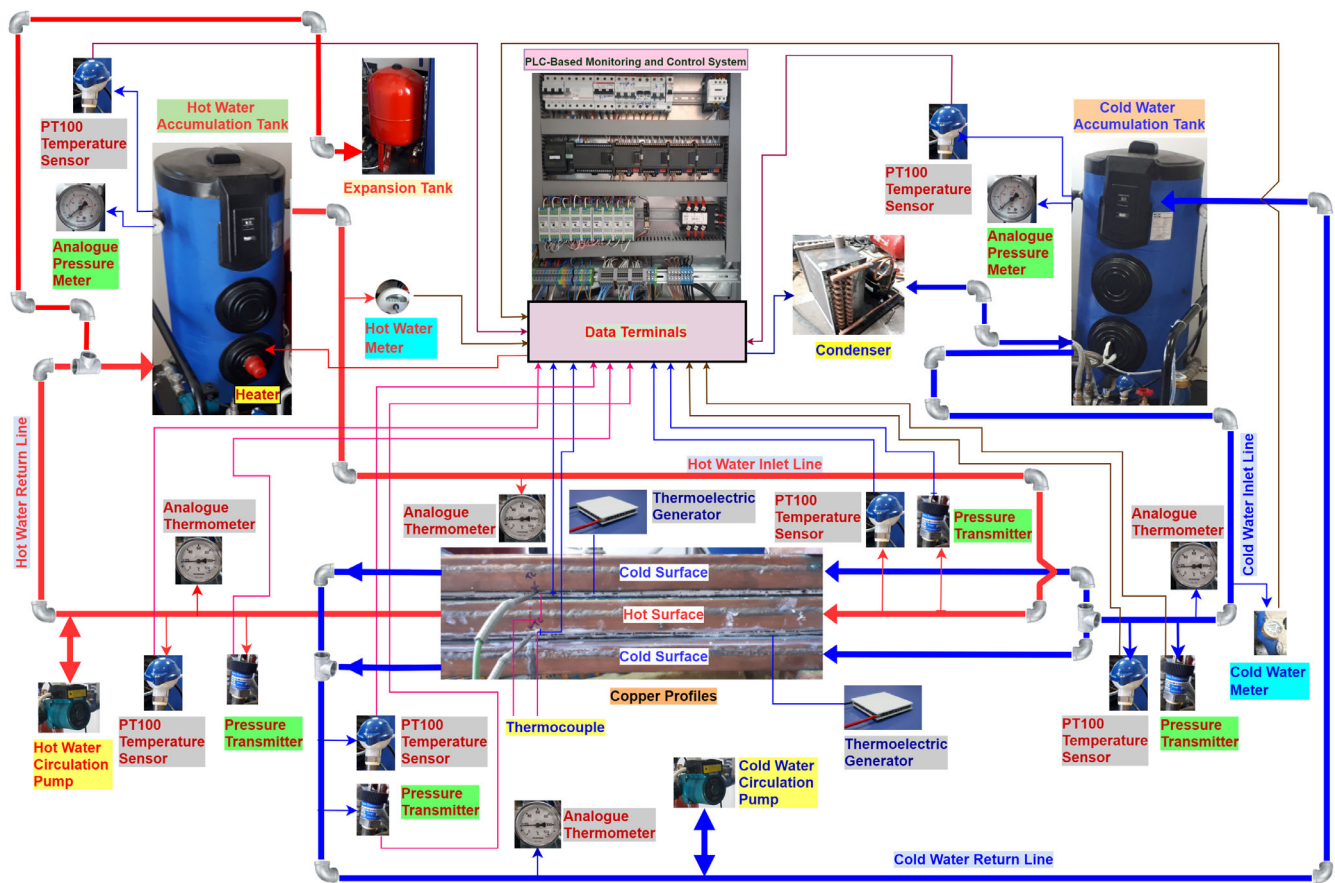


FIGURE 6 The detailed view of the experimental setup

Cold water passes through the profiles located in the upper and lower parts of the copper profile group shown in three separate blocks in Figure 6. Hot water passes

through the copper profile in the middle of the profile group. Here, the copper profiles are produced in the form of closed boxes for transferring the temperature of the

TABLE 2 Main components of the experimental setup

Device type in Figure 6	Device model	Device function	Number of devices
TEG	Kryotherm TGM-199-1.4-0.8	To generate DC electricity from temperature difference	48
PLC-Based Monitoring and Control System (PMCS)	OEM	Control and data acquisition	1
Hot water accumulation tank	Unmak UAT-100 (100 L, with a heater)	To store and heat water	1
Cold water accumulation tank	Unmak UAT-100 (100 L)	To store cold water	1
Copper profile	OEM	To make a thermal difference between two surfaces of a TEG	3
Condenser	Azak Ltd.-1 HP-2.350 kcal-2100 kPa	To cool the water	1
Expansion tank	Wates-50 L-1000 kPa	To prevent excessive pressure in the hot water system	1
Hot water circulation pump	LEO LRP25-60/130	To circulate hot water in hot water lines	1
Cold water circulation pump	LEO LRP25-60/130	To circulate cold water in cold water lines	1
PT100 temperature sensor (6 mm)	Elimko RT02-1P06-5-2wire Class: B (Length: 5 cm, Diameter: 6 mm)	To measure temperatures of water lines	4
PT100 temperature sensor (9 mm)	Elimko RT02-1 K09-16-2wire Class: B (Length: 16 cm, Diameter: 9 mm)	To measure indoor temperatures of accumulation tanks	2
Thermocouple (K-type)	Elimko E-MI04-1 K20-6-K10-SS-TZ (Length: 6 cm, Diameter: 2 mm)	To measure temperatures of hot and cold surfaces of TEG system	3
Pressure transmitter	Atek BCT-110-4B-V-G1/4-C-S30 (0-400 kPa)	To measure pressures of water lines	4
Hot water meter	Apator Powogaz JS-130-10-01-NK (0.1-130°C)	To measure water use in hot water lines	1
Cold water meter	Maddalena SpA DS TRP (0.1-30°C)	To measure water use in cold water lines	1
Analogue thermometer	Pakkens 0-120°C	To monitor temperatures of water lines	2
Analogue pressure meter	Pakkens 0-1000 kPa	To monitor pressures of accumulation tanks	2
Water line	OEM	To carry hot and cold water	1
Valve	OEM	To adjust the water flow manually	2

Abbreviations: OEM, original Equipment Manufacturer; PLC, programmable logic controller; PMCS, based monitoring and control system; TEG, thermoelectric generator.

water passing through them to the TEGs and providing the desired temperature values on the hot and cold surfaces of the TEGs. Kryotherm TGM-199-1.4-0.8 model TEGs are placed between copper profiles. Technical specifications of TEGs are introduced in Table 3. Forty-eight TEGs are used in the system such that half of them are between upper and middle copper profiles and the remaining ones are between middle and lower copper profiles.

Hot and cold water accumulation tanks, each with a storage capacity of 100 L, are used to model the power plant production wells and cooling system at a

geothermal power plant site, respectively. The hot water accumulation tank depicted in Figure 6 represents the production well in a real geothermal power plant. As seen in Figure 6, in order to model the temperature of the geothermal fluid in the production well, a heater is integrated into the hot water accumulation tank. The heater unit is a three-phase resistance heater, and its electrical power is 10 kW. The heater can raise the temperature of the water in the accumulation tank up to 100°C, which is required for TEGs used in this study. An expansion tank was added to the experimental setup so as to prevent the hot water system pressure from

TABLE 3 Technical specification of Kryotherm TEG^{34,35}

Parameter	Requirement	Value
Output Power (P_o)	@ $T_h = 100^\circ\text{C}$, $T_c = 20^\circ\text{C}$	3.2 W
Load Voltage (U_{load})	@ $T_h = 100^\circ\text{C}$, $T_c = 20^\circ\text{C}$, for $R_{\text{load}} = R_{\text{ac}}$	2 V
Load Current (I_{load})	@ $T_h = 100^\circ\text{C}$, $T_c = 20^\circ\text{C}$, for $R_{\text{load}} = R_{\text{ac}}$	1.6 A
TEG Internal Resistance (R_{ac})	@ working temperature of 100°C	$1.25 \Omega \pm 10\%$
Heat Resistance (R_t)	With thermal paste application	$0.57 \text{ K/W} \pm 10\%$
Maximum Efficiency (η_{max}) for $R_{\text{load}} = R_{\text{ac}}$	@ working temperature of 100°C ,	2.6%
Dimensions ($W \times L \times H$)	Height tolerance up to $\pm 0.015 \text{ mm}$	$40 \text{ mm} \times 40 \text{ mm} \times 3.2 \text{ mm}$
Maximum Working Temperature (T_{max})	With thermal paste application	200°C

increasing excessively in Figure 6. The cold water accumulation tank represents the cooling system of the geothermal power plant. The temperature of the water in the cold water accumulation tank can be reduced to $+4^\circ\text{C}$ by using the condenser in Figure 6. The hot water and cold water produced by this way are sent to the copper profiles over the water lines by the circulation pumps shown in Figure 6. The water passing through the copper profiles transfers its heat to the profile. Copper profiles transfer their heat to the hot and cold surfaces of TEGs, which are located between copper profiles. TEGs, which have a temperature difference between their two surfaces, thus start to generate DC electrical energy.

Six PT100 temperature sensors are used to measure the fluid temperatures in the experimental setup. Two of them are used to measure the temperature of the water inside the accumulation tanks, two of them for measuring the water temperature at the inlet and outlet of the hot water main line, and the remaining ones are to measure the water temperature at the inlet and outlet of the cold water line. As seen in Figure 6, the temperature of the water in the hot water inlet line entering the copper profiles touched with the hot surfaces of the TEGs is measured by the PT100 temperature sensor mounted at the point where the line enters the copper profile. Similarly, another PT100 is mounted on cold water return line of the copper profiles in touch with the cold surfaces of the TEGs, allowing the temperature of the water in this line to be measured (Figure 6). Two analogue thermometers are also used to monitor the temperature in the hot and cold water lines. There are three separate K-type thermocouples to measure the surface temperatures of TEGs. As seen in Figure 6, the first one is used to measure the cold surface temperature of the TEGs between the copper profiles located at the top and middle. The

second thermocouple is used to measure the hot surface temperature of TEGs between the copper profiles at the middle and bottom. The third thermocouple is used to measure the cold surface temperature of TEGs between the copper profiles at the middle and bottom.

The first of the four pressure transmitters in the experimental setup is mounted to the section where the hot water line enters the copper profiles, the second one to the section where the cold water main line enters the copper profiles, the third one to the section where the hot water line comes out of the copper profiles, and the last one to the section at the copper profile outlet of the cold water main line. Thus, the pressure in the hot and cold water lines is measured continuously.

The pressure in the water lines should not exceed 400 kPa for system safety. The PMCS in the experimental setup monitors instant information from pressure transmitters and disables the system in case the pressure rises dangerously to the limit value. In addition, two analogue pressure meters are installed at the water inlet of the accumulation tanks to monitor system pressure by the operator. Using the hot water meter included in the experimental setup, the amount of water passing through the hot water line can be measured. Similarly, a cold water meter is installed on the cold water line. The analogue values measured by both water meters can be seen on the screens of the water meters in cubic meters.

As seen in Figure 6, data collected by all sensors in the system enter data terminals. Data terminals are the input terminals of the PMCS. The PMCS receives data coming from all pressure and temperature sensors in the system through its data converters. These received data are evaluated online by the PLC. If necessary, the PMCS intervenes in the system to adjust the pressure and temperature.

2.4 | Simulation of the experimental setup

During the design stage of the experimental setup, first of all, the number of TEGs to be used in the system and their optimum connection type are determined. It is aimed to convert the DC voltage to be produced by TEGs into AC electrical energy by using an inverter. The selected inverter has a power of 150 W in accordance with the output power of the TEGs. The inverter output voltage is 230 V/50 Hz. To simulate the system, a code based on Matlab & Simulink is created. The technical specifications (hot surface temperature, cold surface temperature, TEG voltage, TEG current, etc.) of the Kryotherm TEGs to be connected to this inverter are entered in the data entry section of the Matlab & Simulink-based software in Figure 7A. Data entered in the data entry section can be followed numerically from the data monitoring section (Figure 7B). The user can design a TEG System with the values they will enter in the boxes named series-connected TEGs and parallel-connected TEGs in the data entry section. For the TEG system with 150 W output power to be designed, on the software interface, 12 and 4 numbers are entered in the series-connected TEGs and parallel-connected TEGs boxes, respectively. The number of TEGs connected in series and parallel can be changed by the users, and then the desired TEG system can be obtained. As it is seen in Figure 7B, the efficiency of TEG system obtained by the values entered to the simulation software is 2.44%. Since each TEG has 2 V DC output voltage according to Table 3, the total voltage value of 12 TEGs connected in series will be 24 V by Equation (9):

$$U_{DC-s} = n_{TEG} \times U_{DC-TEG} \quad (9)$$

However, this voltage value drops below 20 V when an inverter is connected to the TEG system output terminal. The line current of TEGs connected in series is 1.60 A. Four of these series branches are connected in parallel in the system. Therefore, the total TEG system voltage is 24 V DC. In addition, the system output current is 6.40 A by Equation (10):

$$I_{DC-TEG\text{SYS}} = n_{\text{string}} \times I_{DC-TEG} \quad (10)$$

These voltage and current values are obtained in case of a temperature difference of 80°C between the hot and cold surfaces (for hot surface temperature $T_h = 100^\circ\text{C}$ and cold surface temperature $T_c = 20^\circ\text{C}$).³⁴ According to the number of series- and parallel-connected TEGs entered to the software, the TEG system output voltage

calculated by the software is 19.95 V DC. This value appears voltageGENERator (V) in Figure 7B. Essentially, the important point is that a TEG system can be designed according to the power and the input voltage range of the inverter. By changing the number of series- and parallel-connected TEGs as desired, the user can create a configuration suitable for the desired TEG system output voltage and efficiency.

2.5 | Experiments

After determining the number and configuration of TEGs to be used in the experimental setup, the stage of designing the platforms where these TEGs will be placed has been started. As shown in Table 3, the dimensions of the TEGs are 40 mm × 40 mm × 3.2 mm (W × L × H). Therefore, the width of the platform on which TEGs will be placed should also be at least 40 mm. To place the TEGs, four of the L-type copper profiles are welded to each other to obtain a copper box profile. There will be three pieces of these copper box profiles in the system, whose dimensions will be 80 mm × 1050 mm × 40 mm (W × L × H). Accumulation tanks, each of which has a storage capacity of 100 L, are used to store hot and cold water that will pass through the copper profiles in the experimental setup. The circulation of the water in the accumulation tanks is made by two circulation pumps (each with a power of 96 W). A circulation pump can circulate 58 L of water per minute.³⁶ To keep the water temperature in the cold water accumulation tank constant at 20°C, a condenser with a value of 2350 kcal is used. To increase the temperature of 100 L (100 kg) of water in the hot water accumulation tank from 20°C to 100°C, a resistance heater with the capacity of at least 9.30 kW is needed. Therefore, a resistance heater with a power of 10 kW is chosen. To prevent the sudden pressure increase that may occur in the system with the temperature increase, a 50 L (1,000 kPa) expansion tank³⁷ is used. Since the operating pressure value of the expansion tank is 1000 kPa and the precharge pressure value is 400 kPa, the heater operation setting is made so that the maximum pressure value (400 kPa) of the system is not exceeded.

In the experimental setup, a total of six PT100 temperature sensors of two different types with protection sheath diameters of 6 mm and 9 mm are used for the measurement of fluid temperatures in Figure 6. These two types of sensors are used according to different waterline diameters in the experimental setup. These sensors are in the resistance thermometer class and give resistance values with regard to the temperature changes, in compliance with the DIN43760 standard.³⁸ They can

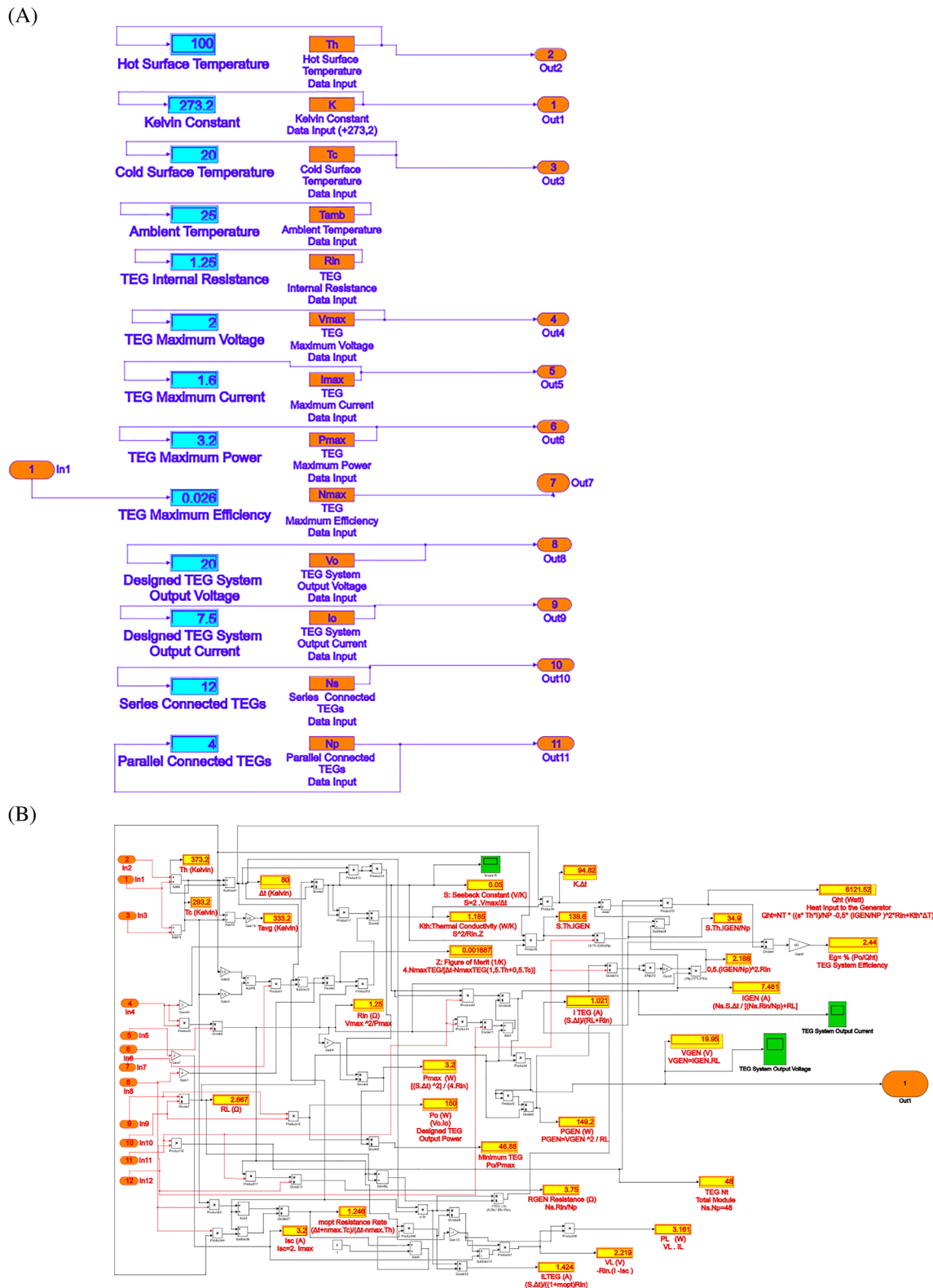


FIGURE 7 A, User interface for data input. B, Output data monitoring interface

work between -200°C and $+850^{\circ}\text{C}$.³⁸ Resistance thermometers give more accurate values at low temperatures than thermocouples.³⁸ For this reason, this type of sensor is preferred for temperature measurements. To monitor

the fluid temperatures, two analog thermometers that can measure between 0°C and 120°C are used in Figure 6. Thermocouples are used to measure the surface temperatures of TEGs between copper profiles in

Figure 6. They have mineral insulation. Thermocouples are preferred in demanding applications where long-term temperature measurement is required due to their flexible structure.³⁹ Mineral insulation (compressed high purity metal-oxide powders) allows equipment measuring wires and metal sheath to be isolated from each other.³⁹ In this context, thermocouples, which are produced according to DIN43710 and IEC60584 standards and can measure up to 1200°C with a high degree of accuracy,³⁹ are used to measure surface temperatures of TEGs. Four pressure transmitters are used to measure hot and cold water fluid pressures in the experimental setup in Figure 6. The selected equipment is piezo-resistive, which can measure up to the upper limit of 400 kPa pressure value in the experimental setup. They can give output voltages in range of 0-10 V DC.⁴⁰ In addition to these pressure transmitters that can send data to the PLC, two analogue pressure meters are shown in Figure 6, which can measure between 0 and 1000 kPa, are also mounted to observe analog values of pressures. To determine the amount of water used in the experiments, two water meters are installed to each of the hot and cold water accumulation tank outlets. The water meter installed to the hot water accumulation tank is a device that can operate at water temperatures of 0.1°C-130°C and can withstand 1600 kPa water pressure.⁴¹ The water meter at the outlet of the cold water accumulation tank has working temperature of 30°C and maximum pressure strength of 1600 kPa.⁴² Both devices are chosen as they are capable of providing the maximum water pressure (400 kPa) and maximum water temperature limits (100°C for hot water and 20°C for cold water) in the system. Three cases with different mass flow rates (0.2, 0.3, and 0.4 kg/s) are considered in the study. In these cases, with the values of 50°C ($T_h = 70^\circ\text{C}$ and $T_c = 20^\circ\text{C}$), 60°C ($T_h = 80^\circ\text{C}$ and $T_c = 20^\circ\text{C}$), 70°C ($T_h = 90^\circ\text{C}$ and $T_c = 20^\circ\text{C}$), and 80°C ($T_h = 100^\circ\text{C}$ and $T_c = 20^\circ\text{C}$) for the temperature differences between hot and cold sides of TEGs, experiments are conducted for 20 minutes with almost constant ambient temperature of 22°C. In Figures 8 and 9, voltage and power output values for three cases and the temperature differences are seen, respectively. Values for 40°C and 90°C are formed by curve fitting.

3 | RESULTS AND DISCUSSION

Some data for the real operating conditions are obtained from the binary cycle geothermal power plant in Denizli, Turkey. For the one module, measured properties of one example for the operating condition at steady state are presented in Table 4.

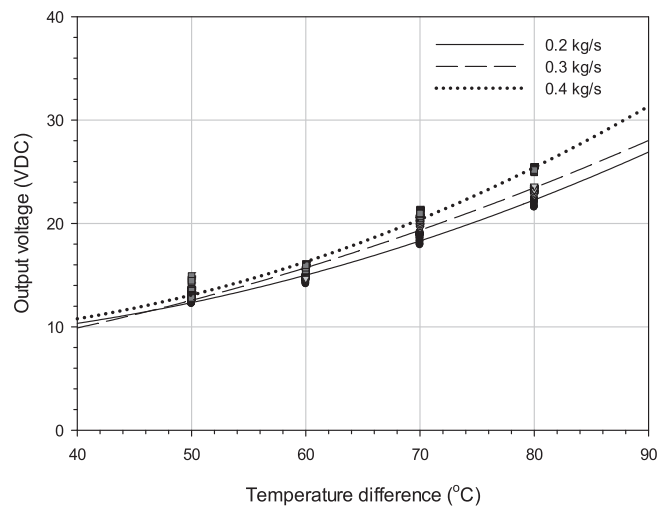


FIGURE 8 Voltage output values for different mass flow rates

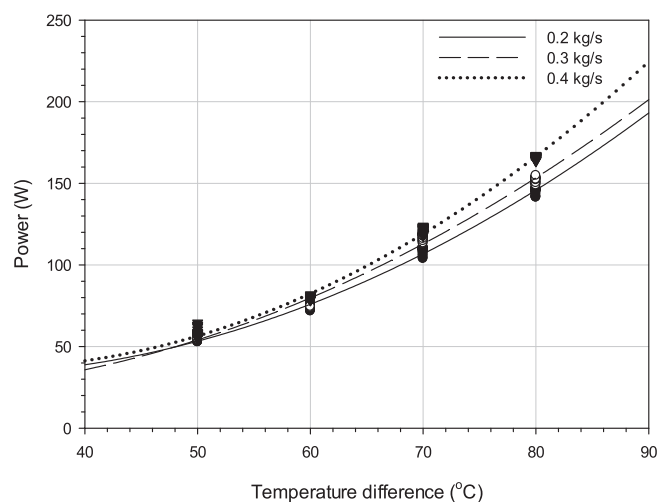


FIGURE 9 Power output values for different mass flow rates

However, they are not enough to evaluate the overall performance of the power plant for different conditions for the reinjection temperature and the temperature of cooling water output. For the geothermal-thermoelectric hybrid power generation system, these temperature values become very important to investigate the temperature differences between the hot and cold sides of TEGs (ΔT) as well as the performance of the geothermal power plant. In the analysis, geothermal brine is considered as water. Engineering Equation Solver (EES) software is utilized for the determination of the thermodynamic properties of the geothermal brine and the working fluid as R245fa. Thermodynamic analysis for each component of the plant and pinch point calculations for the evaporator and condenser are written in EES, so that the parametric analysis using the temperature of the reinjected geothermal brine (T_2) and the inlet temperature of the cooling

water (T_7) as the independent parameters is conducted. For the given example at the steady-state condition above, thermodynamic state properties given in Table 5 are obtained especially for the ORC. Also, by validating with the other real operating conditions and specifications of the module,^{33,43} some other data of the ORC are obtained as shown in Table 6. Effectiveness of the evaporator and the condenser is assumed to be 0.92 and 1, respectively.⁴⁴ Also, efficiency of generator–alternator couple connected to the turbine is assumed to be 0.96.^{33,43}

The inlet temperature of the cooling water (T_7) to the condenser mainly depends on ambient temperature. Therefore, monthly ambient temperature values are obtained from typical meteorological database of Photovoltaic Geographical Information System,⁴⁵ for the years between 2006–2016 at the location of the power plant

TABLE 4 Measured properties of one example for the operating condition at steady state

Properties	Values
Inlet temperature of geothermal brine, T_1 (°C)	103.89
Reinjection temperature of geothermal brine, T_2 (°C)	72.2
Inlet pressure of geothermal brine, P_1 (kPa)	280
Reinjection pressure of geothermal brine, P_2 (kPa)	240
Mass flow rate of geothermal brine, \dot{m}_{GB} (kg.s ⁻¹)	20
Inlet temperature of cooling water, T_7 (°C)	22
Outlet temperature of cooling water, T_8 (°C)	32.8
Inlet pressure of cooling water, P_7 (kPa)	90
Outlet pressure of cooling water, P_8 (kPa)	50
Mass flow rate of cooling water, \dot{m}_{cw} (kg.s ⁻¹)	49.6
Evaporator pressure, P_{ev} (kPa)	735
Condenser pressure, P_{con} (kPa)	216
Gross power, \dot{W}_{gross} (kW)	219
Net power, \dot{W}_{net} (kW)	204

TABLE 5 Thermodynamic state properties of the power plant

Point no	Fluid	T (°C)	P (kPa)	\dot{m} (kg.s ⁻¹)	h (kJ.kg ⁻¹)	s (kJ.kg ⁻¹ .K ⁻¹)
1	Geothermal brine	103.9	280	20	435.6	1.351
2	Geothermal brine	72.2	240	20	302.4	0.9816
3	R245fa	35.98	735	11.53	247.3	1.161
4	R245fa	77.13	735	11.53	459.8	1.778
5	R245fa	45.99	216	11.53	440.8	1.788
6	R245fa	35.69	216	11.53	246.7	1.16
7	Water	22	90	49.6	92.28	0.3246
8	Water	32.8	50	49.6	137.4	0.475

(37° 54' 57" N/28° 52' 48" E). Minimum and maximum ambient temperature values are 6.08°C and 30.83°C in January and July, respectively. Therefore, the inlet temperature values of the cooling water (T_7) are varied from 0°C to 40°C in the parametric analysis. In addition, T_2 values are taken between 40°C and 103.89°C since the temperature of the geothermal brine (T_1) is assumed to be constant at 103.89°C. The outlet temperature values of the cooling water (T_8) are taken as above the inlet temperature of the cooling water (T_7).

Figures 10 and 11 show the variations of the parameters with T_2 values from 40°C to 103.89°C while T_7 , T_8 , and mass flow rate of the geothermal brine are kept constant at 22°C, 32.8°C, and 20 kg/s, respectively. As seen in Figure 10, net power reaches its maximum at 63.98°C with the value of 217.6 kW, and from this point, it is decreasing with the increase in T_2 since thermal energy input from geothermal source (\dot{Q}_{in}) to the evaporator, which is transferred thermal energy to R245fa, becomes less. Also, corresponding evaporator and condenser pressure values for the maximum net power are 596.6 and 216.8 kPa, respectively. Although evaporator pressure rises with T_2 , condenser pressure is almost the same due to the constant T_7 value, 22°C.

In Figure 11, it is seen that mass flow rates of R245fa and the cooling water decline with the increase in T_2 . Carnot and thermal efficiency values increase with the higher T_2 because thermal energy input from geothermal source (\dot{Q}_{in}) and thermal energy output to the condenser (\dot{Q}_{out}) are reducing simultaneously. For the maximum net power from the ORC, mass flow rates of R245fa and the cooling water are calculated to be 14.89 and 63.61 kg/s, and also, Carnot and thermal efficiency values are obtained to be 0.1477 and 0.0638, respectively.

Figures 12 and 13 represent the variations of the parameters with the inlet temperature values of the cooling water (T_7) from 0°C to 40°C while T_1 , T_2 , and mass flow rate of the geothermal brine are kept constant at 103.89°C, 72°C, and 20 kg/s, respectively. In addition,

TABLE 6 Calculated data of the ORC based on the thermodynamic modelling

Properties	Values
Pinch point temperature difference for the evaporator, $\Delta T_{pp,ev}$ (°C)	3.7
Pinch point temperature difference for the condenser, $\Delta T_{pp,con}$ (°C)	3.47
Isentropic efficiency of the turbine, $\eta_{T,s}$	0.85
Isentropic efficiency of the pump, $\eta_{P,s}$	0.75

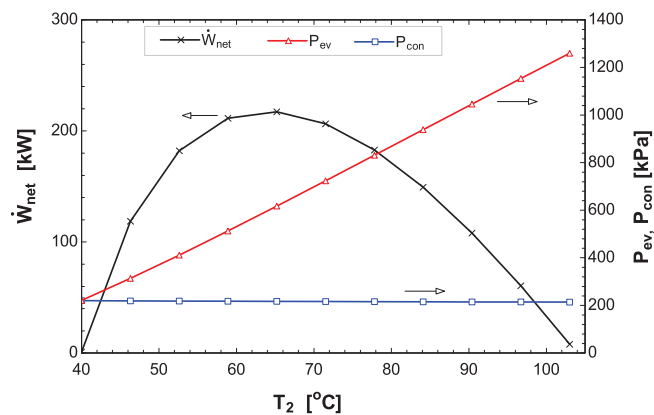


FIGURE 10 Net power, evaporator, and condenser pressure values depending on variable temperature of reinjected geothermal brine

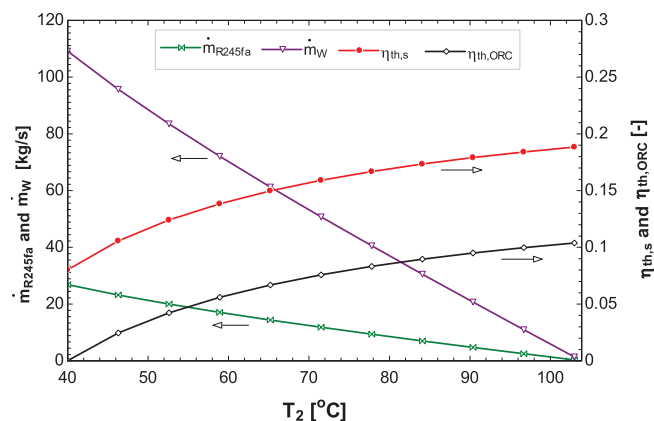


FIGURE 11 Variations of mass flow rates of R245fa and the cooling water and changes in efficiencies with the temperature of reinjected geothermal brine

T_8 is considered as 10°C higher than T_7 . As presented in Figure 12, net power has its maximum value of 260 kW at the minimum T_7 value. With increasing T_7 value, net power is decreasing T_2 due to declining thermal energy output from R245fa to the cooling water via the condenser. Also, this affects the condenser pressure by increasing it, so the condenser pressure determines the

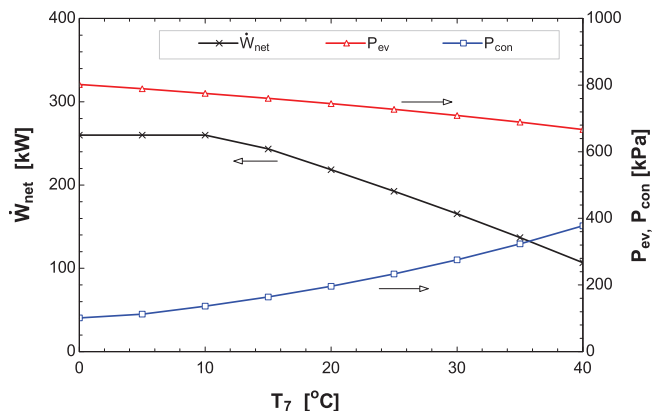


FIGURE 12 Net power, evaporator, and condenser pressure values depending on variable inlet temperature of cooling water

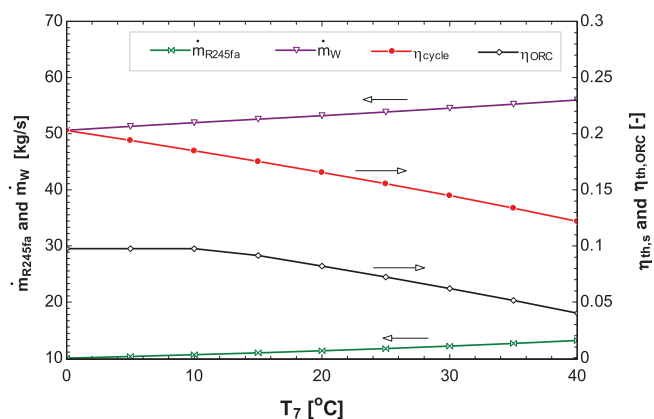


FIGURE 13 Variations of mass flow rates of R245fa and the cooling water and changes in efficiencies with the inlet temperature of cooling water

outlet conditions (pressure and temperature) of the turbine. Although the condenser pressure increases, net power output of the ORC reduces. It has the maximum value of 260 kW at 11.6°C of inlet temperature of cooling water. It can be seen in Figure 13 that mass flow rates of R245fa and the cooling water rise with the increase in T_7 . However, Carnot and thermal efficiency values decrease with the higher T_7 . For the maximum net power from the ORC, mass flow rates of R245fa and the cooling water have their minimum values, which are obtained to be 10.72 and 52.16 kg/s, respectively.

TEGs utilization in the geothermal binary power plant is investigated by using the results obtained from the experimental setup. From the point of view from the heat transfer phenomena, it is very important to determine the temperature drops throughout the geothermal/cooling water pipelines and surface temperatures on hot/cold sides by considering the size of TEGs when they have long and wide layout. However, in this study, only

small power capacity of TEGs with the numbers of 48 is used. Therefore, for the simplicity, temperature drops throughout the geothermal/cooling water pipelines are not taken into account, and surface temperatures on hot/cold sides of TEGs are assumed to be constant along the pipelines where TEGs are mounted. The variations of TEGs power output values with the temperature of reinjected geothermal brine (T_2) and the inlet temperature values of the cooling water (T_7) are shown in Figures 14 and 15, respectively. The corresponding temperature differences between hot and cold sides of TEGs for these situations are also given in these figures. As seen in Figure 14, power output of TEGs increasing with the increase in T_2 . However, for the higher T_2 values after its reaching the maximum value, net power of the ORC reduces. For the maximum net power output of ORC, which is 217.6 kW, TEGs are able to produce 43.42 W for the temperature difference of 41.98°C

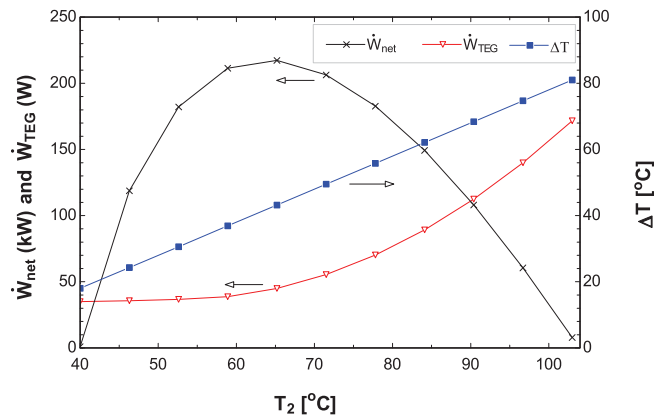


FIGURE 14 Net power, power output of TEGs, and temperature difference with the change of the inlet temperature of reinjected geothermal brine

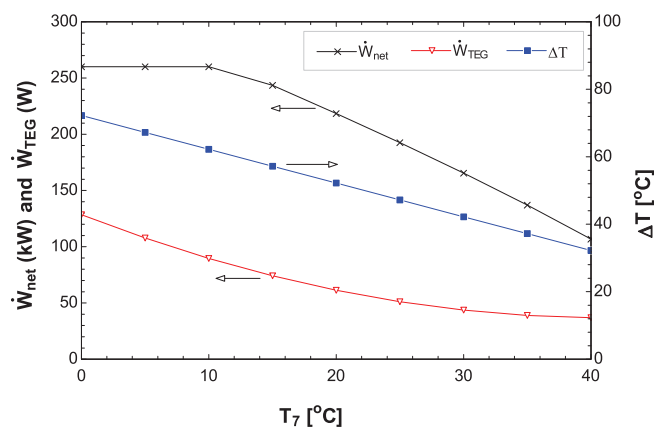


FIGURE 15 Net power, power output of TEGs, and temperature difference with the change of the inlet temperature of cooling water

corresponding to this status. Therefore, for benefiting more energy production from this hybrid energy system, TEGs have to be used with lower power outputs.

In Figure 15, evaluation of power output of TEGs can be seen with the change of T_7 . For the higher T_7 values, net power of the ORC reduces, and also power output of TEGs goes down. For the maximum net power output of ORC, TEGs are able to produce 84.29 W for the temperature difference of 60.6°C. Therefore, utilizing TEGs in the power plant for the lower T_7 values can be considered. In conclusion, it is important to note that increased numbers of TEGs and higher temperature differences do not mean to get the higher net power output of the hybrid energy system since TEGs impact on energy input from geothermal brine (\dot{Q}_{in}) to ORC. Also, cold side temperature of TEGs (inlet temperature of cooling water) is limited to the condenser temperature which mainly depends on ambient temperature. Therefore, utilization of TEGs could have positive and negative effect on net power output. A simultaneously design approach can be considered for using TEGs in any waste heat recovery system to get the optimum numbers/layout configuration of TEGs.

4 | CONCLUSIONS

The aim of this study is to investigate the use of TEGs in the geothermal power plant for recovering the waste heat of reinjected geothermal brine. The main conclusions of the study are listed as follows:

- The numbers of TEGs that are connected in series and parallel were found to be 12 and 4, respectively, for the optimized configuration of TEGs for maximum power output and the relevant voltage stability using Matlab & Simulink.
- From the experimental setup, which was designed for the optimized configuration of TEGs, it was found that it is possible to heat to electrical conversion efficiencies of TEGs up to 2.44%.
- Three cases with different mass flow rates (0.2, 0.3, and 0.4 kg/s) are considered in the study. In these cases, it was found that higher mass flow rates and temperature differences increase the voltage and power outputs with values of 50°C ($T_h = 70^\circ\text{C}$ and $T_c = 20^\circ\text{C}$), 60°C ($T_h = 80^\circ\text{C}$ and $T_c = 20^\circ\text{C}$), 70°C ($T_h = 90^\circ\text{C}$ and $T_c = 20^\circ\text{C}$), and 80°C ($T_h = 100^\circ\text{C}$ and $T_c = 20^\circ\text{C}$) for the temperature differences between the hot and cold sides of TEGs.
- However, in the real operating conditions of the geothermal power plant, the TEGs should be used carefully to generate more efficient electrical energy from

such a hybrid energy system. The parametric energy analysis revealed that the power output of TEGs increases with the rise in temperature of the reinjected geothermal brine, but the net power of the ORC decreases. For the maximum net power output of ORC, which is 217.6 kW, TEGs are able to produce 43.42 W for the temperature difference of 41.98°C that corresponds to this status. Moreover, for the high inlet temperature values of cooling water, the net power of the ORC decreases, and the power output of the TEGs also goes down. TEGs are able to produce 84.29 W for the temperature difference of 60.6°C for the ORC's maximum net power output of 260 kW.

For the future work, an adaptive control system for the variable load characteristics will be implemented in the system to control the hot water flow rate, and the response of the system can then be investigated. Also, comprehensive energy, exergy, and thermo-economic analyses of the system have been planned to determine the inefficiencies and the improvement potential of the hybrid system.

ACKNOWLEDGEMENT

This study was supported by the Scientific Research Coordination Unit of Pamukkale University under the project number 2017FEBE027. The authors would like to thank Pamukkale University for its support with this study. The authors also would like to thank JEODEN Electric Production Inc., Denizli-Turkey, for giving the opportunity to examine its geothermal power plant site and for sharing the power plant data.

NOMENCLATURE

Symbols

\dot{E}_{in}	energy inlet per unit time, kJ.s^{-1}
\dot{E}_{out}	energy outlet per unit time, kJ.s^{-1}
h	specific enthalpy, kJ.kg^{-1}
$h_{pp,con}$	specific enthalpy at pinch point of condenser, kJ.kg^{-1}
$h_{pp,ev}$	specific enthalpy at pinch point of evaporator, kJ.kg^{-1}
h_1	specific enthalpy of geothermal brine, kJ.kg^{-1}
h_2	specific enthalpy of reinjected geothermal brine, kJ.kg^{-1}
h_3	specific enthalpy of working fluid at the inlet of evaporator, kJ.kg^{-1}
h_4	specific enthalpy of working fluid at the outlet of evaporator, kJ.kg^{-1}
h_{4f}	specific enthalpy of saturated working fluid at the outlet of evaporator, kJ.kg^{-1}

h_5	specific enthalpy of working fluid at the outlet of turbine, kJ.kg^{-1}
h_6	specific enthalpy of working fluid at the outlet of condenser, kJ.kg^{-1}
h_{6g}	specific enthalpy of vaporized working fluid at the outlet of condenser, kJ.kg^{-1}
h_7	specific enthalpy of cooling water at the inlet of condenser, kJ.kg^{-1}
h_8	specific enthalpy of cooling water at the outlet of condenser, kJ.kg^{-1}
I_{DC-TEG}	output current of a TEG, A
$I_{DC-TEGS}$	output current of a TEG system, A
I_{load}	load current, A
\dot{m}_{GB}	mass flow rate of geothermal brine, kg.s^{-1}
\dot{m}_{in}	inlet mass flow rate, kg.s^{-1}
\dot{m}_{out}	outlet mass flow rate, kg.s^{-1}
\dot{m}_{R245fa}	mass flow rate of R245fa, kg.s^{-1}
\dot{m}_{CW}	mass flow rate of cooling water, kg.s^{-1}
n_{string}	string number in parallel connected
n_{TEG}	number of TEGs connected in series
P_o	output power, W
P_1	inlet pressure of geothermal brine, kPa
P_2	reinjection pressure of geothermal brine, kPa
P_7	inlet pressure of cooling water, kPa
P_8	outlet pressure of cooling water, kPa
P_{con}	condenser pressure, kPa
P_{ev}	evaporator pressure, kPa
\dot{Q}_{in}	thermal energy input per unit time, kJ.s^{-1}
\dot{Q}_{out}	thermal energy output per unit time, kJ.s^{-1}
R_{ac}	internal TEG resistance, Ω
R_t	heat resistance, K.W^{-1}
s	specific entropy, $\text{kJ.kg}^{-1}.\text{K}^{-1}$
T_1	inlet temperature of geothermal brine, °C
T_2	reinjection temperature of geothermal brine, °C
T_3	temperature of working fluid at the inlet of evaporator, °C
T_4	temperature of working fluid at the outlet of evaporator, °C
T_5	temperature of working fluid at the outlet of turbine, °C
T_6	temperature of working fluid at the outlet of condenser, °C
T_7	inlet temperature of cooling water, °C
T_8	outlet temperature of cooling water, °C
T_c	TEG cold side temperature, °C
T_h	TEG hot side temperature, °C
T_{max}	maximum working temperature, °C
$T_{pp,con}$	pinch point temperature of condenser, °C
$T_{pp,ev}$	pinch point temperature of evaporator, °C
U_{DC-s}	DC line voltage of TEGs connected in series, V
U_{DC-TEG}	DC voltage of a TEG, V

U_{load}	load voltage, V
\dot{W}_{gross}	gross power, kW
\dot{W}_{net}	net power, kW



Greek Symbols

\mathcal{E}_{con}	effectiveness of condenser
\mathcal{E}_{ev}	effectiveness of evaporator
η_{max}	maximum efficiency, %
$\eta_{\text{P,s}}$	isentropic efficiency of the pump
$\eta_{\text{T,s}}$	isentropic efficiency of the turbine
ΔT	temperature difference, °C
$\Delta T_{\text{pp,con}}$	pinch point temperature difference for the condenser, °C
$\Delta T_{\text{pp,ev}}$	pinch point temperature difference for the evaporator, °C

Abbreviations

AC	Alternative current
CFD	Computational fluid dynamics
DC	Direct current
EES	Engineering Equation Solver
OEM	Original Equipment Manufacturer
ORC	Organic Rankine cycle
PLC	Programmable Logic Controller
PMCS	PLC-Based Monitoring and Control System
TEG	Thermoelectric generator

ORCID

Mahmut Hekim  <https://orcid.org/0000-0002-2766-1023>
Engin Cetin  <https://orcid.org/0000-0002-0368-3631>

REFERENCES

- IPCC. Summary for Policymakers. *Global Warming of 1.5°C*; Geneva, Switzerland: The Intergovernmental Panel on Climate Change (IPCC); 2018.
- IEA. *Electricity Market Report*. Paris, France: IEA Publications; 2020.
- IRENA. *Geothermal Power: Technology Brief*; 2017.
- REN21. *Renewables 2020 Global Status Report*; 2020.
- IEA. *Geothermal Tracking Report*. <https://www.iea.org/reports/geothermal>, (accessed March 2021).
- Zarrouk SJ, Moon H. Efficiency of geothermal power plants: a worldwide review. *Geothermics*. 2014;51:142-153.
- Habibollahzade A, Houshfar E, Ashjaee M, Ekrafi K. Continuous power generation through a novel solar/geothermal chimney system: technical/cost analyses and multi-objective particle swarm optimization. *J Clean Prod*. 2021;283:1-18.
- Hu S, Yang Z, Li J, Duan Y. Thermo-economic optimization of the hybrid geothermal-solar power system: a data-driven method based on lifetime off-design operation. *Energy Convers Manag*. 2021;229:1-17.
- Ozturk M, Dincer I. Development of a combined flash and binary geothermal system integrated with hydrogen production for blending into natural gas in daily applications. *Energy Convers Manag*. 2021;227:1-8.
- Heidarnejad P, Genceli H, Asker M, Khanmohammadi S. A comprehensive approach for optimizing a biomass assisted geothermal power plant with freshwater production: techno-economic and environmental evaluation. *Energy Convers Manag*. 2020;226:1-17.
- Loni R, Najafi G, Bellos E, Rajaei F, Said Z, Mazlan M. A review of industrial waste heat recovery system for power generation with organic Rankine cycle: recent challenges and future outlook. *J Clean Prod*. 2021;287:1-28.
- Hribernik A, Hribernik TM. Techno-economic model for a quick preliminary feasibility evaluation of organic Rankine cycle applications. *J Sustain Dev Energy Water Environ Syst*. 2021;9:1-18.
- Quoilin S. Sustainable energy conversion through the use of organic rankine cycles for waste heat recovery and solar applications [PhD thesis]. University of Liège; 2011.
- Lecompte S, Huisseune H, Broek M, Vanslambrouck B, Paepe M. Review of organic Rankine cycle (ORC) architectures for waste heat recovery. *Renew Sust Energ Rev*. 2015;47:448-461.
- Li D, He Z, Wang Q, Wang X, Wu W, Xing Z. Thermodynamic analysis and optimization of a partial evaporating dual-pressure organic Rankine cycle system for low-grade heat recovery. *Appl Therm Eng*. 2021;185:1-16.
- Madruga S. Modeling of enhanced micro-energy harvesting of thermal ambient fluctuations with metallic foams embedded in phase change materials. *Renew Energy*. 2021;168:424-437.
- Mahfuz MMH, Tomita M, Hirao S, et al. Designing a bileg silicon-nanowire thermoelectric generator with cavity-free structure. *Jpn J Appl Phys*. 2021;60:1-6.
- Ahiska R, Mamur H, Ullis M. Modelling and experimental study of thermoelectric module as generator. *J Fac Eng Archit Gazi Univ*. 2011;26:889-896.
- Niu X, Yu J, Wang S. Experimental study on low-temperature waste heat thermoelectric generator. *J Power Sources*. 2009;188:621-626.
- Suter C, Jovanovic ZR, Steinfeld A. A 1 kW_e thermoelectric stack for geothermal power generation – modeling and geometrical optimization. *Appl Energy*. 2012;99:379-385.
- Liu C, Chen P, Li K. A 500 W low-temperature thermoelectric generator: design and experimental study. *Int J Hydrog Energy*. 2014;39:15497-15505.
- Ahiska R, Mamur H. Design and implementation of a new portable thermoelectric generator for low geothermal temperatures. *IET Renew Power Gener*. 2013;7:700-706.
- Ahiska R, Mamur H. Development and application of a new power analysis system for testing of geothermal thermoelectric generators. *Int J Green Energy*. 2016;13(7):672-681.
- Gholamian E, Habibollahzade A, Zare V. Development and multi-objective optimization of geothermal-based organic Rankine cycle integrated with thermoelectric generator and proton exchange membrane electrolyzer for power and hydrogen production. *Energy Convers Manag*. 2018;174:112-125.
- Khanmohammadi S, Saadat-Targhi M, Ahmed FW, Afrand M. Potential of thermoelectric waste heat recovery in a combined geothermal, fuel cell and organic Rankine flash cycle (thermodynamic and economic evaluation). *Int J Hydrog Energy*. 2020;45:6934-6948.

26. Catalan L, Aranguren P, Araiz M, Perez G, Astrain D. New opportunities for electricity generation in shallow hot dry rock fields: a study of thermoelectric generators with different heat exchangers. *Energy Convers Manag.* 2019;200:1-11.
27. Catalan L, Araiz M, Aranguren P, Astrain D. Computational study of geothermal thermoelectric generators with phase change heat exchangers. *Energy Convers Manag.* 2020;221:1-15.
28. Neamtu MO, Trip ND, Burca AT. Low Power Renewable Energy System used for Power Back-up Applications. *IEEE 23rd International Symposium for Design and Technology in Electronic Packaging.* Romania, October 26–29, 2017.
29. Catalan L, Araiz M, Aranguren P, et al. Prospects of autonomous volcanic monitoring stations: experimental investigation on thermoelectric generation from fumaroles. *Sensors.* 2020;20:1-21.
30. Ding T, Liu J, Shi K, Hu S, Yang H. Theoretical study on geothermal power generation using thermoelectric technology: a potential way to develop geothermal energy. *Int J Green Energy.* 2021;18:297-307.
31. Cetin E, Hekim M, Ozden H, & Bozkurt MA. A small scale geothermal power plant in Denizli-Turkey for sustainable energy studies. *26th European Conference on Operational Research.* Italy, July 1–4, 2013.
32. Bozkurt MA. *Investigation of the Effects of Drilling Well and Fluid Properties on Electricity Generation in Geothermal Power Plants.* BSc thesis: Pamukkale University; 2013.
33. Pratt & Whitney. *Hot Liquid to Electricity Power System Product Data and Application Guide.* USA; 2009.
34. Kryotherm. *Specification of Generating Thermoelectric Modules TGM-199-1.4-0.8.* Russia; 2019.
35. Kryotherm. *Introduction into Thermoelectric Power Generation.* Russia; 2019.
36. LEO. *LRP Circulation Pump Data Sheet.* China; 2020.
37. Wates. *Expansion Tank Data Sheet.* Turkey; 2020.
38. Elimko. *Resistance Thermometers Data Sheet.* Turkey; 2020.
39. Elimko. *Mineral Insulated Thermocouples.* Turkey; 2020.
40. Atek. *BCT-110 Piezoresistive Pressure Sensor Data Sheet.* Turkey; 2020.
41. Apator Powogaz. *Vane wheel water meters operating instructions.* Poland; 2018.
42. Maddalena. *DS TRP Water Meter Data Sheet.* Italy; 2020.
43. SUMEC GeoPower. *PureCycle Model 280 ORC.* <http://www.sumecgeopower.com/en/46/technology/orchhigh-speed-turbine-pure-cycle>, (accessed March 2021).
44. Boyd T, DiPippo R. Technical assessment of the combined heat and power plant at the Oregon institute of technology, Klamath Falls. *Oregon GRC Trans.* 2012;36:1143-1149.
45. PVGIS. *EU Photovoltaic Geographical Information System.* https://re.jrc.ec.europa.eu/pvg_tools/en/#TMY, (accessed March 2021).

How to cite this article: Hekim M, Cetin E. Energy analysis of a geothermal power plant with thermoelectric energy harvester using waste heat. *Int J Energy Res.* 2021;45(15):20891-20908. <https://doi.org/10.1002/er.7145>